

# Language Models as Semantic Teachers: Post-Training Alignment for Medical Audio Understanding

Tsai-Ning Wang, Lin-Lin Chen, Neil Zeghidour, and Aaqib Saeed

**Abstract**—Pre-trained audio models excel at detecting acoustic patterns in auscultation sounds but often fail to grasp their clinical significance, limiting their use and performance in diagnostic tasks. To bridge this gap, we introduce AcuLa (Audio–Clinical Understanding via Language Alignment), a lightweight post-training framework that instills semantic understanding into any audio encoder by aligning it with a medical language model, which acts as a “semantic teacher.” To enable alignment at scale, we construct a large-scale dataset by leveraging off-the-shelf large language models to translate the rich, structured metadata accompanying existing audio recordings into coherent clinical reports. Our alignment strategy combines a representation-level contrastive objective with a self-supervised modeling, ensuring that the model learns clinical semantics while preserving fine-grained temporal cues. AcuLa achieves state-of-the-art results across 18 diverse cardio-respiratory tasks from 10 different datasets, improving the mean AUROC on classification benchmarks from 0.68 to 0.79 and, on the most challenging COVID-19 cough detection task, boosting the AUROC from 0.55 to 0.89. Our work demonstrates that this audio-language alignment transforms purely acoustic models into clinically-aware diagnostic tools, establishing a novel paradigm for enhancing physiological understanding in audio-based health monitoring.

**Index Terms**—Audio understanding, Large language models, Cross-modal alignment, Knowledge distillation

## I. INTRODUCTION

Existing audio encoders capture subtle temporal and spectral patterns in auscultation sounds but still lack explicit clinical semantics. This capability gap renders them “semantically blind,” limiting their utility in high-stakes diagnostic tasks. This creates a fundamental paradox: while large language models (LLMs) possess deep, contextual knowledge of medical terminology like “systolic murmurs” or “wheezes,” this understanding remains disconnected from the audio models that process the raw signals. Digital stethoscopes and other sensors may capture a wealth of acoustic data, but without a bridge to semantic meaning, this information remains under-utilized.

Multimodal contrastive learning, popularized by frameworks like CLIP [1], aims to bridge such divides by aligning heterogeneous modalities in a shared embedding space. This approach has enabled powerful cross-modal retrieval and classification capabilities. However, these methods often suffer from a persistent ‘modality gap,’ where embeddings from different sources form distinct clusters,

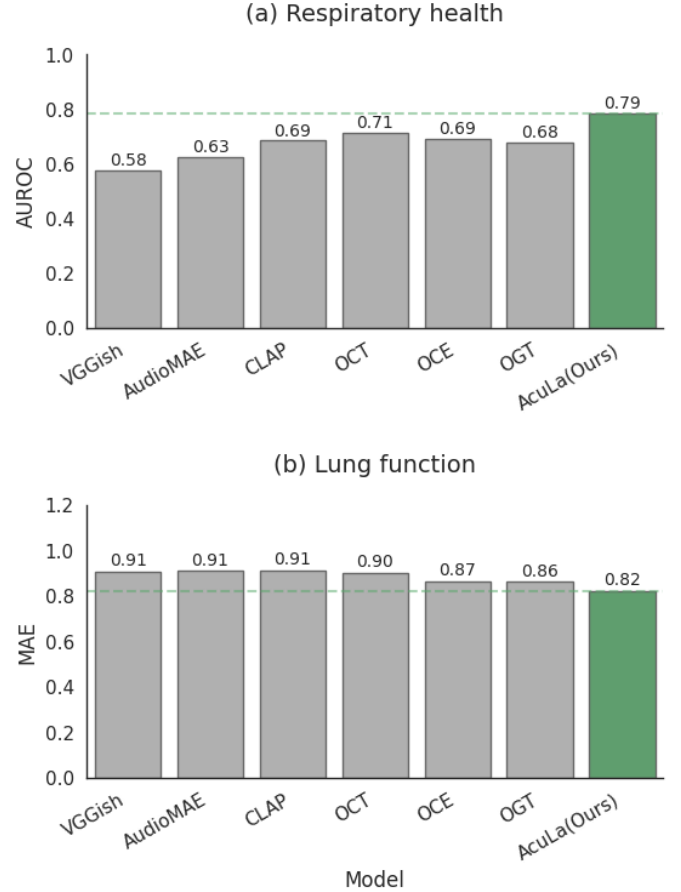


Fig. 1: Performance comparison of audio-based models. (a) Average AUROC for respiratory classification tasks (T1-T9). (b) Average MAE for lung function estimation tasks (T10-T16). Our model (pink) outperforms all baselines, achieving the highest AUROC (0.79) and lowest MAE (0.82).

hindering fine-grained alignment and interpretability [2], [3]. This issue is particularly acute in clinical applications, where subtle acoustic variations carry significant diagnostic weight and demand precise semantic grounding.

While existing methods have sought to bridge this gap through architectural modifications [4], auxiliary objectives [5], or post-training alignment [6], their focus has been on aligning two perceptual modalities. Even recent advances in knowledge transfer, such as [7], operate under this paradigm, enhancing language models by injecting knowledge from vision models. These approaches share a common directional assumption: knowledge flows from concrete perception to abstract representation. Our work fundamentally diverges by

Tsai-Ning Wang and Lin-Lin Chen are with Eindhoven University of Technology, The Netherlands (e-mail: t.n.wang@tue.nl; l.chen@tue.nl).

Neil Zeghidour is with Kyutai, France (e-mail: neil@kyutai.org).

Aaqib Saeed is with the Eindhoven University of Technology, The Netherlands and the Eindhoven Artificial Intelligence Systems Institute, The Netherlands. (e-mail: a.saeed@tue.nl).

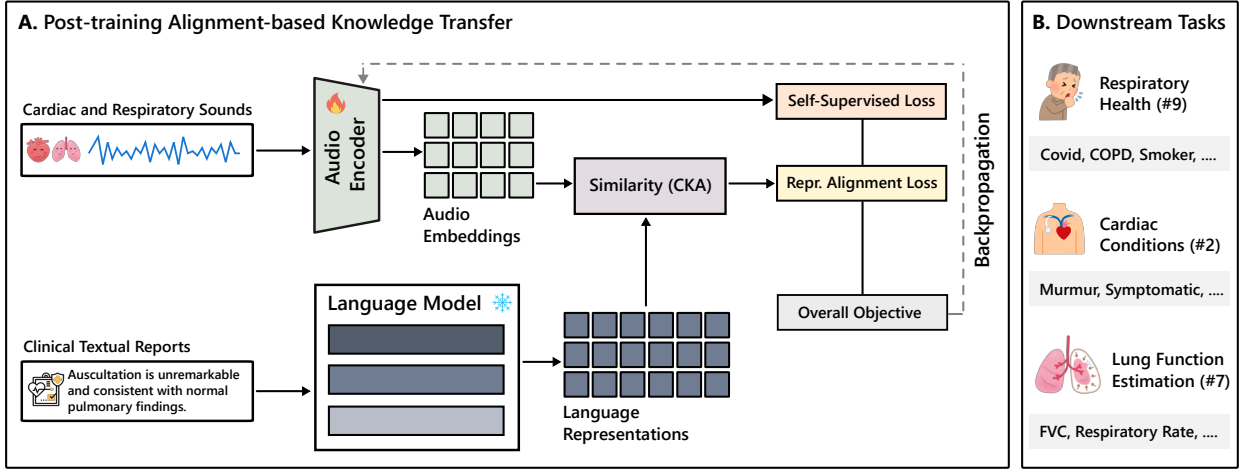


Fig. 2: Architecture of the audio-language alignment framework. (A) Audio encoders extract features from clinical recordings, which are aligned with language representations via similarity matching. (B) Down-stream tasks enabled by the aligned model, including (i) respiratory-health classification (9 tasks), (ii) cardiac-condition detection (2 tasks) and (iii) lung-function estimation (7 tasks).

framing the problem not as mutual alignment, but as a directed and asymmetric knowledge infusion. We investigate how to leverage the vast, pre-existing semantic knowledge of an LLM, treating it as a “semantic teacher” to guide and enrich a specialized “acoustic student.” This presents a distinct challenge: grounding high-level clinical concepts from text into the fine-grained, temporal patterns of a raw audio signal, a problem unexplored by prior methods.

This frontier is especially important for domains rich with temporal and semantic information, such as medical audio. Millisecond-scale events like the onset of a lung crackle or the specific timing of a heart murmur contain precise clinical information that current audio-only models struggle to link to a diagnosis. To address this, we introduce AcuLa (Audio–Clinical Understanding via Language Alignment), a general, post-training framework that instills clinical semantic understanding into any pre-trained audio encoder. In our approach, a frozen, LLM acts as a ‘semantic teacher,’ guiding an audio ‘student’ model to map acoustic patterns to their corresponding clinical meanings.

We demonstrate AcuLa’s effectiveness in the challenging domain of cardio-respiratory health (see Figure 1). By synthetically generating a large-scale dataset of clinical reports from structured metadata, we create the necessary paired data to align audio recordings with their clinical interpretations. Our results show that this alignment transforms standard audio encoders into clinically-aware models that can better differentiate subtle pathologies and significantly improves downstream tasks performance.

Our work makes the following key contributions:

- **Model-Agnostic Audio-Language Knowledge Transfer:** We propose a general framework (AcuLa) to enhance pre-trained audio encoders by transferring knowledge from LLMs. This demonstrates a novel paradigm where LLMs serve as semantic teachers for specialized auditory models (see Figure 2 for an overview).
- **Preservation-Focused Teacher-Student Design:** Our lightweight architecture connects pre-trained models

through minimal projection layers, preserving specialized knowledge in both models while enabling efficient cross-modal knowledge transfer without expensive retraining or architectural modifications.

- **Synthetic Data Generation from Structured Meta-data:** We construct paired audio-text data by generating clinical auscultation reports ( $\approx 100,000$ ) from real meta-data of audio clip using powerful off-the-shelf LLMs, producing semantically accurate and diverse narratives aligned with each recording.
- **Dual Objective Optimization:** We combine a representation alignment loss with audio self-supervised modeling (such as masked acoustic reconstruction loss) in a multi-task setting. This dual objective ensures that the model learns semantic relationships while maintaining the fine-grained temporal precision essential for medical audio analysis.

## II. RELATED WORK

### A. Medical Audio Analysis

The analysis of respiratory and cardiac sounds has traditionally been a unimodal task. Supervised deep learning models have shown success in disease classification given sufficient expert-labeled data, while self-supervised pre-training on large, unannotated corpora has proven effective in low-resource settings [8]. Recognizing the limitations of audio-only analysis, recent efforts have started to incorporate textual features. For instance, RespLLM [9] fuses spectral features with clinical notes via cross-modal attention. However, such approaches typically treat audio and text as separate processing streams, fusing them only at a late stage for a final decision. This shallow integration prevents the audio encoder itself from learning a semantically rich representation, limiting its ability to ground acoustic events in clinical meaning. Our work moves beyond late fusion by directly aligning audio and language representations at a deep feature level.

## B. Cross-Modal Alignment

Bridging the semantic gap between modalities is a central challenge in machine learning. Existing methods can be broadly understood through the lens of their alignment strategies.

**Representation Alignment.** The dominant paradigm, popularized by CLIP [1], learns a shared embedding space where corresponding pairs from different modalities are projected to be close. This contrastive approach has been successfully extended to the audio domain with models like CLAP [10] and AudioCLIP [11], enabling better cross-modal learning. However, these frameworks often struggle with a “modality gap,” where representations remain clustered by their original modality, hindering fine-grained understanding [2]. This limitation is particularly critical for medical signals, where subtle pattern differences are diagnostically vital.

**Knowledge Transfer and Distillation.** An alternative perspective is to view alignment as a form of directed knowledge transfer. This can be achieved through various mechanisms. Generative methods like AudioLM [12] and AudioGen [13] learn to synthesize audio conditioned on text, implicitly learning a shared structure. Knowledge distillation [14] transfers representations from a “teacher” to a “student” network mostly focusing on supervised task-specific models. Most relevant to our work is regularization-based alignment, where a model’s representation space is regularized to match that of another. CMAR [7], for example, regularizes an LLM’s latent space using features from a vision model. Recent connector-based approaches for speech–text learning [15], [16] instead focus on token-level correspondences, training cross-modal adapters or attention modules end to end and often updating the language model itself. These methods require paired audio–text data and emphasize fine-grained synchronous alignment. In contrast, our setting targets post-training global embedding alignment: the medical LLM remains frozen, and lightweight projection heads align encoder representations under schema-constrained, clip-level textual supervision.

**Our Contributions and Positioning.** Despite these advances, two critical gaps remain. First, within medical audio, a deep, semantic alignment between audio representations and clinical text is underexplored. Second, in the broader field of cross-modal learning, knowledge transfer has been almost exclusively studied from perceptual domains, like vision to language, or between static modalities like images and text, with few attempts at unifying audio like ImageBind [17]. AcuLa is the first work to bridge both gaps. We introduce a framework for deep representation alignment specifically for temporal medical audio. Crucially, we invert the conventional direction of knowledge transfer, using a pre-trained LLM as a semantic teacher to instill clinical understanding into a specialized audio encoder, directly addressing the challenges of grounding abstract semantics in time-varying signals.

## III. METHODOLOGY

Our framework, **AcuLa**, establishes a post-training alignment between a pre-trained audio encoder and a pre-trained language model. We achieve this by introducing lightweight,

trainable projection heads and fine-tuning the audio encoder, guided by a dual objective that promotes semantic similarity while retaining fine-grained acoustic detail. The core language model remains frozen, acting as a fixed semantic teacher.

### A. Problem Statement

Let  $\mathcal{A}_\theta$  be a pre-trained audio encoder with parameters  $\theta$ , and  $\mathcal{L}_\phi$  be a pre-trained language model with parameters  $\phi$ . Given a batch of  $B$  paired examples  $\{(\mathbf{x}_i, \mathbf{r}_i)\}_{i=1}^B$ , where  $\mathbf{x}_i \in \mathbb{R}^{T \times F}$  is an audio spectrogram and  $\mathbf{r}_i$  is the corresponding textual report, our goal is to learn parameters for an audio projection head  $P_{\psi_a}^{\text{audio}}$  and a language projection head  $P_{\psi_l}^{\text{language}}$ . Let  $\psi = \{\psi_a, \psi_l\}$  be the set of all trainable projection parameters. These heads map the outputs of their respective encoders into a shared  $d$ -dimensional embedding space:

$$\mathbf{h}_i^{\text{audio}} = P_{\psi_a}^{\text{audio}}(\mathcal{A}_\theta(\mathbf{x}_i)) \in \mathbb{R}^d \quad (1)$$

$$\mathbf{h}_i^{\text{language}} = P_{\psi_l}^{\text{language}}(\mathcal{L}_\phi(\mathbf{r}_i)) \in \mathbb{R}^d \quad (2)$$

The learning objective is to optimize the audio encoder parameters  $\theta$  and the projection parameters  $\psi$  such that (i) the representations  $\mathbf{h}_i^{\text{audio}}$  and  $\mathbf{h}_i^{\text{language}}$  for corresponding pairs are semantically aligned, while (ii) the audio encoder’s ability to model detailed acoustic patterns is preserved. The LLM parameters  $\phi$  remain frozen throughout.

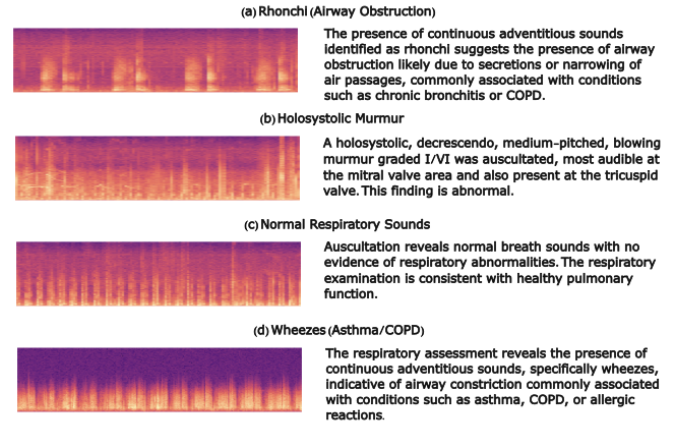


Fig. 3: Spectrograms of cardiopulmonary sounds with paired clinical reports. (a) Rhonchi showing continuous adventitious sounds from airway obstruction. (b) Holosystolic murmur indicating mitral valve pathology. (c) Normal breath sounds with clear pulmonary function. (d) Wheezes revealing airway constriction associated with asthma or COPD.

### B. Alignment Architecture

Our architecture (Figure 2.A) is designed to be lightweight and preservation-focused. The core components are the audio encoder  $\mathcal{A}_\theta$  and the language model  $\mathcal{L}_\phi$ . The knowledge transfer is mediated by two simple, trainable projection heads,  $P_{\psi_a}^{\text{audio}}$  and  $P_{\psi_l}^{\text{language}}$ , implemented as multi-layer perceptrons (MLPs). This design enables efficient alignment while minimizing disruption to the pre-trained models architectures.

### C. Training Objective

Our multi-task training objective is designed to simultaneously achieve semantic alignment and preserve the temporal fidelity of the audio encoder. The full objective is a weighted sum of two losses:

$$\mathcal{L}(\theta, \psi) = \lambda_{\text{align}} \mathcal{L}_{\text{align}}(\theta, \psi; \phi) + \lambda_{\text{SSM}} \mathcal{L}_{\text{SSM}}(\theta) \quad (3)$$

Here, we optimize the audio encoder parameters  $\theta$  and the projection head parameters  $\psi$ , while the LLM parameters  $\phi$  remain frozen.

**Semantic Alignment via Centered Kernel Alignment (CKA).** To align the two modalities, we require a robust similarity metric between the sets of batch embeddings,  $\mathbf{H}^{\text{audio}} = [\mathbf{h}_1^{\text{audio}}, \dots, \mathbf{h}_B^{\text{audio}}]^T$  and  $\mathbf{H}^{\text{language}} = [\mathbf{h}_1^{\text{language}}, \dots, \mathbf{h}_B^{\text{language}}]^T$ . We use Centered Kernel Alignment (CKA) [18], a metric that compares the geometric structure of representation spaces, making it invariant to isotropic scaling and rotation. CKA is defined via the Gram matrices of the mean-centered representations,  $\mathbf{G}^{\text{audio}} = \bar{\mathbf{H}}^{\text{audio}T} \bar{\mathbf{H}}^{\text{audio}}$  and  $\mathbf{G}^{\text{language}} = \bar{\mathbf{H}}^{\text{language}T} \bar{\mathbf{H}}^{\text{language}}$ .

$$\mathcal{A}(\mathbf{H}^{\text{audio}}, \mathbf{H}^{\text{language}}) = \frac{\langle \mathbf{G}^{\text{audio}}, \mathbf{G}^{\text{language}} \rangle_F}{\|\mathbf{G}^{\text{audio}}\|_F \|\mathbf{G}^{\text{language}}\|_F} \quad (4)$$

where  $\langle \cdot, \cdot \rangle_F$  is the Frobenius inner product. The alignment loss seeks to maximize this similarity:

$$\mathcal{L}_{\text{align}}(\theta, \psi; \phi) = 1 - \mathcal{A}(\mathbf{H}^{\text{audio}}, \mathbf{H}^{\text{language}}) \quad (5)$$

**Acoustic Preservation via Self-Supervised Modeling (SSM).** The alignment loss alone could cause the audio encoder to discard acoustic information not present in the simplified text reports, a phenomenon known as representation collapse [19]. To counteract this and preserve fine-grained temporal details, we incorporate the audio encoder’s self-supervised objective,  $\mathcal{L}_{\text{SSM}}$ . For many state-of-the-art audio models, this is a masked acoustic modeling loss [20], which involves reconstructing masked patches of the input spectrogram or contrastive objective [21]. In our case, they act as a powerful regularizer, ensuring the audio representations do not catastrophically forget their core acoustic modeling capabilities. The final optimization thus becomes:

$$\theta^*, \psi^* = \arg \min_{\theta, \psi} [\lambda_{\text{align}} \mathcal{L}_{\text{align}}(\theta, \psi; \phi) + \lambda_{\text{SSM}} \mathcal{L}_{\text{SSM}}(\theta)] \quad (6)$$

This dual objective balances the acquisition of new semantic knowledge with the preservation of existing acoustic capabilities.

### D. Synthetic Alignment Data Generation

A significant challenge in medical multimodal learning is the scarcity of large-scale, paired audio-text datasets. To overcome this, we devise a scalable strategy to generate high-quality clinical text from existing audio datasets with structured metadata. We leverage an off-the-shelf LLM, GPT-4o [22], to synthesize clinical reports. For each audio recording from public datasets like ICBHI [23] and Circor [24], we compile its available metadata—patient demographics, recording conditions, and diagnostic labels (e.g., presence of crackles/wheezes)—into a structured prompt (see Appendix A

TABLE I: Statistics of the our synthesized data used for model alignment. For **UK Covid-19**, **IC+EX** denotes the union of *Induced Cough* (IC) and *Exhalation* (EX). Duration values show average duration in seconds.

Dataset	Modality	#Reports	#Audio	Avg. Duration (s)
ICBHI	Lung sound	6,899	6,899	22.2
HFLung	Lung sound	9,765	10,554	15.0
UK Covid-19	IC+EX	72,999	40,252	5.9
CoughVID	Induced cough	11,314	7,179	6.9
Circor	Heart sound	1,568	5,282	22.87
SPRSound	Lung sound	1,772	2,496	11.15
ZCHSound	Heart sound	1,259	1,259	20.06

TABLE II: Downstream task characteristics grouped by task category. Abbreviations: Exhal. = Exhalation, Obstr. = Obstructive, Resp. = Respiratory, Sam. = Samples, Sub. = Subjects.

Dataset	Task	Modality	#Sam. (#Sub.)	Data Distribution
UK COVID-19	Covid/Non-covid	Exhal.	2500 (2500)	840/1660
	Covid/Non-covid	Cough	2500 (2500)	840/1660
CoughVID	Covid/Non-covid	Cough	6175 (n/a)	547/5628
	Female/Male	Cough	7263 (n/a)	2468/4795
ICBHI	COPD/Healthy	Lung sounds	828 (90)	793/35
	Smoker/Non-smoker	Cough	948 (n/a)	201/747
Coswara	Female/Male	Cough	2496 (n/a)	759/1737
	Obstr./Healthy	Lung sounds	234 (79)	129/105
KAUH Resp.@TR	COPD severity	Lung sounds	504 (42)	72/60/84/84/204
MMLung	FVC	Deep breath	40 (40)	3.402 ± 1.032 L
	FEV1	Deep breath	40 (40)	2.657 ± 0.976 L
	FEV1/FVC	Deep breath	40 (40)	0.808 ± 0.190 L
	FVC	O Vowels	40 (40)	3.402 ± 1.032 L
	FEV1	O Vowels	40 (40)	2.657 ± 0.976 L
	FEV1/FVC	O Vowels	40 (40)	0.808 ± 0.190 L
NoseMic	Respiratory rate	Breath	1297 (16)	13.915 ± 3.386 bpm
Circor	Murmur/Healthy	Heart Sounds	1568 (n/a)	1144/ 424
	Symptomatic/Healthy	Heart Sounds	1259 (n/a)	693/566

and Figure 3). The LLM is tasked to act as a clinical specialist (e.g., a pulmonologist) and generate a concise, natural-language report based *only* on the provided information. With precise and explicit prompting of LLM, we ensure factual grounding while encouraging linguistic diversity. Examples of metadata–report pairs are provided in Appendix B. This process yields a corpus of over 100,000 paired audio-report samples, summarized in Table I.

## IV. EXPERIMENTS

We conduct a comprehensive set of experiments to validate the effectiveness of our proposed framework, AcuLa. We first detail the baseline models against which we compare, followed by the implementation details for AcuLa, and finally outline our rigorous evaluation protocol for all downstream tasks.

### A. Baselines

To situate AcuLa’s performance, we compare it against a diverse set of strong pre-trained models representing different architectural and training paradigms. These include VGGish, AudioMAE [20], and CLAP [10]. We also include the OPERA family of models (generative and contrastive both) [8], which are foundation models trained specifically on respiratory audio. As a non-deep-learning benchmark, we use OpenSMILE [25] to extract a standard set of hand-crafted acoustic features. For all deep learning baselines, we use the authors’ official pre-trained encoders to extract features. Unless otherwise

TABLE III: AUROC ( $\uparrow$ ) on health condition inference tasks (higher is better). The best model for each task is highlighted. We report mean and standard deviation from five independent runs. All baseline results (VGGish, AudioMAE, CLAP, OCT, OCE, OGT) are reported in [8].  $\checkmark$  denotes when our method outperforms the OpenSmile baseline (detailed in Appendix C), while \* indicates superior performance compared to all other pretrained models.

ID	Task	VGGish	AudioMAE	CLAP	OCT	OCE	OGT	AcuLa (Ours)
T1	Covid (Exhale)	0.580 $\pm$ 0.001	0.549 $\pm$ 0.001	0.565 $\pm$ 0.001	0.586 $\pm$ 0.008	0.551 $\pm$ 0.010	0.605 $\pm$ 0.001	<b>0.698 <math>\pm</math> 0.001</b> $\checkmark$ *
T2	Covid (Cough)	0.557 $\pm$ 0.005	0.616 $\pm$ 0.001	0.648 $\pm$ 0.003	0.701 $\pm$ 0.002	0.629 $\pm$ 0.006	0.677 $\pm$ 0.001	<b>0.730 <math>\pm</math> 0.008</b> $\checkmark$ *
T3	Covid (Cough)	0.538 $\pm$ 0.028	0.554 $\pm$ 0.004	0.599 $\pm$ 0.007	0.578 $\pm$ 0.001	0.566 $\pm$ 0.008	0.552 $\pm$ 0.003	<b>0.887 <math>\pm</math> 0.003</b> $\checkmark$ *
T4	Gender (Cough)	0.600 $\pm$ 0.001	0.628 $\pm$ 0.001	0.665 $\pm$ 0.001	0.795 $\pm$ 0.001	0.721 $\pm$ 0.001	0.735 $\pm$ 0.000	<b>0.796 <math>\pm</math> 0.004</b> $\checkmark$ *
T5	COPD (Lung)	0.605 $\pm$ 0.077	0.886 $\pm$ 0.017	<b>0.933 <math>\pm</math> 0.005</b>	0.855 $\pm$ 0.012	0.872 $\pm$ 0.011	0.741 $\pm$ 0.011	0.826 $\pm$ 0.014 $\checkmark$
T6	Smoker (Cough)	0.507 $\pm$ 0.027	0.549 $\pm$ 0.022	0.680 $\pm$ 0.009	0.685 $\pm$ 0.012	0.674 $\pm$ 0.013	0.650 $\pm$ 0.005	<b>0.830 <math>\pm</math> 0.011</b> $\checkmark$ *
T7	Gender (Cough)	0.606 $\pm$ 0.003	0.724 $\pm$ 0.001	0.742 $\pm$ 0.001	<b>0.874 <math>\pm</math> 0.000</b>	0.801 $\pm$ 0.002	0.825 $\pm$ 0.001	0.845 $\pm$ 0.004 $\checkmark$
T8	Obstructive (Lung)	0.605 $\pm$ 0.036	0.616 $\pm$ 0.041	0.697 $\pm$ 0.004	0.722 $\pm$ 0.016	0.741 $\pm$ 0.014	0.703 $\pm$ 0.016	<b>0.752 <math>\pm</math> 0.019</b> $\checkmark$ *
T9	COPD severity (Lung)	0.590 $\pm$ 0.034	0.510 $\pm$ 0.021	0.636 $\pm$ 0.045	0.625 $\pm$ 0.038	0.683 $\pm$ 0.007	0.606 $\pm$ 0.015	<b>0.710 <math>\pm</math> 0.028</b> $\checkmark$ *

TABLE IV: MAE ( $\downarrow$ ) on lung function estimation tasks (lower is better). Best model per task is highlighted. We report mean and standard deviation across subjects. All baseline results (VGGish, AudioMAE, CLAP, OCT, OCE, OGT) are from [8].  $\checkmark$  denotes when our method outperforms the OpenSmile baseline (detailed in Appendix C), while \* indicates superior performance compared to all other pretrained models.

ID	Task	VGGish	AudioMAE	CLAP	OCT	OCE	OGT	AcuLa (Ours)
T10	FVC (Breath)	0.904 $\pm$ 0.568	0.900 $\pm$ 0.551	0.896 $\pm$ 0.542	0.924 $\pm$ 0.583	<b>0.848 <math>\pm</math> 0.607</b>	0.892 $\pm$ 0.618	0.865 $\pm$ 0.575 $\checkmark$
T11	FEV1 (Breath)	0.839 $\pm$ 0.563	0.821 $\pm$ 0.590	0.840 $\pm$ 0.547	0.837 $\pm$ 0.563	0.834 $\pm$ 0.581	0.825 $\pm$ 0.560	<b>0.742 <math>\pm</math> 0.565</b> $\checkmark$ *
T12	FEV1/FVC (Breath)	0.131 $\pm$ 0.146	0.129 $\pm$ 0.146	0.134 $\pm$ 0.146	0.128 $\pm$ 0.140	0.132 $\pm$ 0.141	0.128 $\pm$ 0.141	<b>0.127 <math>\pm</math> 0.142</b> $\checkmark$ *
T13	FVC (Vowel)	0.895 $\pm$ 0.559	0.883 $\pm$ 0.588	0.883 $\pm$ 0.560	0.885 $\pm$ 0.553	<b>0.761 <math>\pm</math> 0.544</b>	0.878 $\pm$ 0.550	0.779 $\pm$ 0.553 $\checkmark$
T14	FEV1 (Vowel)	0.842 $\pm$ 0.559	0.876 $\pm$ 0.561	0.859 $\pm$ 0.541	0.780 $\pm$ 0.542	0.830 $\pm$ 0.561	0.774 $\pm$ 0.554	<b>0.725 <math>\pm</math> 0.540</b> $\checkmark$ *
T15	FEV1/FVC (Vowel)	0.130 $\pm$ 0.145	0.131 $\pm$ 0.141	0.137 $\pm$ 0.147	0.132 $\pm$ 0.140	0.136 $\pm$ 0.150	0.130 $\pm$ 0.138	<b>0.123 <math>\pm</math> 0.142</b> $\checkmark$ *
T16	Breathing Rate	2.605 $\pm$ 0.759	2.641 $\pm$ 0.813	2.650 $\pm$ 0.947	2.636 $\pm$ 0.858	2.525 $\pm$ 0.782	2.416 $\pm$ 0.885	<b>2.388 <math>\pm</math> 0.835</b> $\checkmark$ *

specified, AcuLa is applied to the OPERA (GT) encoder to demonstrate its enhancement capabilities.

### B. Implementation Details

Our implementation of AcuLa employs MedGemma-4B [26] as the default language model ( $\mathcal{L}_\phi$ ), which has been pre-trained on medical literature, and utilizes the OPERA encoder [8] as the audio foundation model ( $\mathcal{A}_\theta$ ). To bridge the modality gap, we introduce two MLP projection heads. The audio projection MLP maps the 384-dimensional OPERA features to a 512-dimensional shared space via a two-layer network ( $384 \rightarrow 1024 \rightarrow 512$ ) with ReLU activation and 20% dropout. The language projection MLP similarly transforms the 2048-dimensional MedGemma-4B hidden states to the same 512-dimensional space.

During the alignment phase, audio inputs are preprocessed into 8-second segments sampled at 16kHz and converted to log-mel spectrograms with 64 mel bins. We apply on-the-fly data augmentation using the AugLy [27] library, randomly selecting one transformation per sample from a set including a 5dB volume increase, amplitude normalization, low-pass filtering (300Hz cutoff), or high-pass filtering (3000Hz cutoff). We train the model using the AdamW optimizer, applying a learning rate of  $1 \times 10^{-5}$  to both the audio encoder and the projection heads. We train for 50 epochs with a linear learning rate schedule incorporating 400 warmup steps. The batch size is set to 24, with gradient accumulation over 2 steps to fit within memory constraints. The combined loss function weights the CKA-based alignment loss and the SSM loss equally ( $\lambda_{\text{align}} = \lambda_{\text{MAM}} = 1.0$ ). The entire alignment process takes approximately 30 hours on a single NVIDIA A100 GPU.

### C. Downstream Tasks and Evaluation Protocol

**Downstream Tasks.** We evaluate all models on a challenging benchmark of 18 downstream tasks (figure 2B), primarily sourced from the OPERA benchmark [8] and expanded with additional cardiac sound datasets. As detailed in Table II, these tasks cover three distinct clinical areas: respiratory health classification, lung function regression, and cardiac condition classification.

**Evaluation Protocol.** To ensure a fair and direct comparison of representation quality, we employ a standardized linear probing methodology across all models. We first extract fixed, d-dimensional embeddings for all audio clips in a given task using the respective frozen encoder. Subsequently, a lightweight supervised prediction head is trained on these static embeddings. This protocol ensures that performance differences are directly attributable to the intrinsic quality of the learned representations with our approach rather than the nuances of fine-tuning.

The prediction head is a simple shallow network, either a single linear layer or a one-hidden-layer MLP. Its architecture is selected as a hyperparameter for each task using the same settings as OPERA [8] for consistency. It is trained using the Adam optimizer with an initial learning rate of  $10^{-4}$  and an  $L_2$  penalty. The learning rate is decayed by a factor of 0.97 after each epoch. We employ an early stopping criterion, halting training if the validation metric fails to improve for five consecutive epochs and retaining the checkpoint with the best validation performance for testing.

For classification tasks, we report the mean and standard deviation of the Area Under the Receiver Operating Characteristic Curve (AUROC) over five independent runs with



TABLE V: Comparison of audio encoders after alignment with MedGemma-4B [OPERA, CLAP, AudioMAE] and Qwen 2.5-Omni-7B. T1–T9: respiratory classification [AUROC ( $\uparrow$ ), higher = better]. T10–T16: lung-function estimation [MAE ( $\downarrow$ ), lower = better]. Numbers in brackets give *absolute* changes vs. the baseline of the same backbone. Improvements are highlighted in **green**. ++ indicates AcuLa enhanced semantic alignment improves upon pre-trained encoders.

ID	Task	OGT++	OCT++	OCE++	CLAP++	AudioMAE++	Qwen-Omni++
T1	Covid / Non-covid (Exhalation)	0.698 [+9.3]	0.684 [+9.8]	0.657 [+10.6]	0.665 [+10.0]	0.673 [+12.4]	0.664 [+7.3]
T2	Covid / Non-covid (Cough)	0.730 [+5.3]	0.750 [+4.9]	0.690 [+6.1]	0.702 [+5.4]	0.716 [+10.0]	0.703 [+3.7]
T3	Covid / Non-covid (Cough)	0.887 [+33.5]	0.864 [+28.6]	0.860 [+29.4]	0.890 [+29.1]	0.862 [+30.8]	0.807 [+21.4]
T4	Female / Male (Cough)	0.796 [+6.1]	0.804 [+0.9]	0.733 [+1.2]	0.725 [+6.0]	0.758 [+13.0]	0.750 [+0.7]
T5	COPD / Healthy (Lung)	0.826 [+8.5]	0.883 [+2.8]	0.887 [+1.5]	0.891 [−4.2]	0.847 [−3.9]	0.794 [+2.1]
T6	Smoker / Non-smoker (Cough)	0.830 [+18.0]	0.827 [+14.2]	0.821 [+14.7]	0.760 [+8.0]	0.794 [+24.5]	0.786 [+10.6]
T7	Female / Male (Cough)	0.845 [+2.0]	0.868 [−0.6]	0.802 [+0.1]	0.794 [+5.2]	0.822 [+9.8]	0.779 [−0.5]
T8	Obstructive / Healthy (Lung)	0.752 [+4.9]	0.722 [+0.0]	0.748 [+0.7]	0.742 [+4.5]	0.746 [+13.0]	0.724 [+0.0]
T9	COPD severity (Lung)	0.710 [+10.4]	0.714 [+8.9]	0.728 [+4.5]	0.718 [+8.2]	0.699 [+18.9]	0.665 [+7.4]
T10	FVC (Breath)	0.865 [−0.027]	0.896 [−0.028]	0.842 [−0.006]	0.893 [−0.003]	0.892 [−0.008]	0.912 [−0.021]
T11	FEV <sub>1</sub> (Breath)	0.742 [−0.083]	0.753 [−0.084]	0.750 [−0.084]	0.775 [−0.065]	0.781 [−0.040]	0.785 [−0.063]
T12	FEV <sub>1</sub> /FVC (Breath)	0.127 [−0.001]	0.129 [+0.001]	0.138 [+0.006]	0.136 [+0.002]	0.138 [+0.009]	0.132 [+0.001]
T13	FVC (Vowel)	0.779 [−0.099]	0.785 [−0.100]	0.775 [+0.014]	0.812 [−0.071]	0.825 [−0.058]	0.836 [−0.075]
T14	FEV <sub>1</sub> (Vowel)	0.725 [−0.049]	0.731 [−0.049]	0.770 [−0.060]	0.766 [−0.093]	0.751 [−0.125]	0.768 [−0.037]
T15	FEV <sub>1</sub> /FVC (Vowel)	0.123 [−0.007]	0.125 [−0.007]	0.137 [+0.001]	0.139 [+0.002]	0.129 [−0.002]	0.141 [−0.005]
T16	Breathing Rate	2.388 [−0.028]	2.605 [−0.031]	2.494 [−0.031]	2.495 [−0.155]	2.426 [−0.215]	2.480 [−0.023]

TABLE VI: AUROC ( $\uparrow$ ) on nine respiratory-classification tasks. Columns use the abbreviations Exh. (exhalation), Cgh. (cough), and COPD sev. (COPD severity). **Baselines** (left block) are reported in [8]. **AcuLa (Zero-shot)**: our retrieval-and-similarity pipeline that classifies each test clip without seeing any task labels. **AcuLa**: a task-specific *logistic-regression probe* trained on frozen AcuLa embeddings, following the linear probing protocol described in Section IV-C.

Model	Covid			Gender		COPD		Smoker		Gender		Obstructive		COPD sev.		Avg.
	Exh.	Cgh.1	Cgh.2	Cgh.	Lung	Cgh.	Cgh.	Cgh.	Lung	Cgh.	Lung	Lung	Lung	Lung	Lung	
VGGish	0.580	0.557	0.538	0.600	0.605	0.507	0.606	0.605	0.590	0.576						0.576
AudioMAE	0.549	0.616	0.554	0.628	0.886	0.549	0.724	0.616	0.510	0.626						0.626
CLAP	0.565	0.648	0.599	0.665	0.933	0.680	0.742	0.697	0.636	0.685						0.685
OCT	0.586	0.701	0.578	0.795	0.855	0.685	0.874	0.722	0.625	0.713						0.713
OCE	0.551	0.629	0.566	0.721	0.872	0.674	0.801	0.741	0.683	0.693						0.693
OGT	0.605	0.677	0.552	0.735	0.741	0.650	0.825	0.703	0.606	0.677						0.677
AcuLa	0.698	0.730	0.887	0.796	0.826	0.830	0.845	0.752	0.710	0.786						0.786
AcuLa (Zero-shot)	0.602	0.665	0.768	0.683	0.789	0.755	0.714	0.702	0.656	0.704						0.704

different random seeds to ensure robustness. For regression tasks, which often feature smaller datasets with few unique subjects, we adopt a more rigorous Leave-One-Subject-Out cross-validation strategy. In this setup, the model is trained to minimize Mean Absolute Error (MAE), and we report the average MAE across all held-out subjects.

**Zero-shot classification.** In addition to the linear probe evaluation above, we assess AcuLa in a fully *zero-shot* regime (Table VI). For each test clip we (i) extract its frozen embedding, (ii) retrieve the top-5 clinical reports from the FAISS [28] text index built on the train set embeddings, (iii) embed the retrieved report together with the task’s class names using JINA (text model) [29], and (iv) assign the class whose text embedding has the highest cosine similarity to the report embedding. No task-specific weights are learned; the entire pipeline uses our alignment model.

## V. RESULTS

We present a detailed analysis of AcuLa’s performance, demonstrating its effectiveness across a wide range of clinical tasks. Our results show that by infusing audio encoders with semantic knowledge from LLMs, AcuLa consistently enhances their diagnostic capabilities.

### A. Performance on Downstream Clinical Tasks

We evaluate AcuLa against a suite of strong baselines on 18 downstream tasks. The results, summarized in Tables III and IV, show that AcuLa achieves state-of-the-art performance across respiratory classification, lung function regression, and cardiac classification tasks.

**Respiratory Health Condition Classification.** In the nine classification tasks (Table III), AcuLa demonstrates superior performance, showing a clear advantage in identifying pathological conditions from audio signals. We see highest improvements in tasks that require nuanced acoustic discrimination. For instance, in COVID-19 detection from cough sounds

TABLE VII: Average performance across task categories for different LLMs. Respiratory-condition inference uses AUROC  $\uparrow$  (higher = better), lung-function estimation uses MAE  $\downarrow$  (lower = better), and cardiac-condition inference uses AUROC  $\uparrow$  (higher = better). Detailed per-task results are provided in Appendix E, Table XII.

Task Category	#	Llama-3.2-3B [30]	DS-R1-DQ-1.5B [31]	Helium 2B [32]	SmolLM2 [33]	MedGemma-4B [26]
Respiratory health $\uparrow$	9	0.731	0.702	0.692	0.668	<b>0.786</b>
Lung function $\downarrow$	7	0.853	0.896	0.907	0.928	<b>0.821</b>
Cardiac condition $\uparrow$	2	0.639	0.658	0.604	0.636	<b>0.661</b>

(T3), AcuLa improves the AUROC to 0.887, a substantial gain over the next-best baseline and far exceeding traditional methods like OpenSMILE (0.537 AUROC). This suggests that the semantic guidance from the LLM helps the model distinguish subtle, clinically significant variations in coughs that purely acoustic models miss. Similarly, major gains in smoker identification (T6) and COPD-related tasks (T5, T8, T9) indicate that AcuLa effectively learns to associate specific acoustic biomarkers with their underlying clinical labels. Even on tasks like gender classification (T4, T7), where acoustic cues are already strong, AcuLa maintains a competitive edge, confirming that the semantic alignment enhances, rather than compromises, the model’s inherent discriminative power.

**Lung Function Regression.** AcuLa also sets a new standard in all seven lung function estimation tasks, achieving the lowest Mean Absolute Error (MAE) in every case (Table IV). The improvements are particularly strong for tasks involving sustained phonation (T13-T15), where a semantic understanding of vocal effort and respiratory capacity is most beneficial. Here, AcuLa substantially reduces prediction errors for FVC and FEV1, likely because the LLM’s knowledge helps the model interpret how vocal patterns correlate with physiological lung parameters. While the gains on breath-based spirometry tasks (T10-T12) are more modest, they are consistent across all metrics, showing the broad applicability of our approach. The improved accuracy in breathing rate estimation (T16) further underscores AcuLa’s enhanced ability to extract physiologically meaningful information from complex respiratory sounds.

**Generality and Model-Agnosticism** A core contribution of our work is that AcuLa is a general framework applicable to any pre-trained audio encoder. To validate this, we apply our post-training alignment procedure to a diverse set of encoders, including the OPERA family, CLAP, AudioMAE, and the audio encoder of a general multimodal model, Qwen2.5-Omni [34]. The results, presented in Table V, are unequivocal. Regardless of the underlying architecture or original training paradigm, our alignment method consistently and significantly boosts performance. For example, OPERA-based models see large gains in cough-based tasks, while the general-purpose AudioMAE and CLAP models become much more effective at clinical classification after alignment. Even when applied to the audio encoder from Qwen2.5-Omni [34], which was not pre-trained on medical data, AcuLa yields competitive results, demonstrating its power to instill domain-specific semantics. This strong and consistent improvement across various backbones confirms that AcuLa is a versatile and model-agnostic framework for enhancing clinical audio understanding.

**Zero-shot respiratory classification.** Table VI shows that AcuLa’s zero-shot pipeline performs competitively across nine respiratory tasks, often rivaling or exceeding the best audio-only baselines (VGGish, AudioMAE, CLAP, OCT, OCE, OGT), despite using no task-specific labels. In several tasks (e.g., Smoker, Covid), the retrieval-based approach demonstrates clear advantages. Further adding a lightweight linear probe to the frozen AcuLa features yields an additional 4–12 pp absolute AUROC gain, leading to new state-of-the-art results on most tasks. See Appendix D for examples of the retrieval outputs.

## B. Ablation Studies and Analysis

To understand the key components of AcuLa’s success and validate our design choices, we conduct a series of comprehensive ablation studies. We analyze the impact of the language model choice, the training data composition, and the specific mechanisms of our alignment strategy.

### Choice of Semantic Teacher (LLM).

First, we investigate how the choice and size of the LLM teacher affect performance. Table VII shows a comparison of five different language models. The domain-specialized MedGemma-4B model consistently provides the best results across all three task categories. This highlights the value of leveraging an LLM with deep, pre-existing medical knowledge, particularly for nuanced classification tasks where it achieves a mean AUROC of 0.786. Interestingly, while smaller, general-purpose models are less effective, their performance on regression tasks suggests that basic linguistic competence is sufficient for capturing some physiologically relevant correlations. However, for high-stakes clinical tasks, a domain-aware teacher is clearly superior than general LLMs.

**Domain-Specific Training** Table VIIIa examines the impact of training exclusively on respiratory sounds. While respiratory task performance marginally improves (0.788 vs 0.786 AUROC), cardiac performance degrades (0.601 vs 0.661 AUROC). This trade-off demonstrates that diverse acoustic training enables better cross-domain generalization, even when the primary application domain is well-represented in the training data. Per-task results for this respiratory-only adaptation are reported in Appendix F.

**Impact of Training Data.** Next, we analyze the influence of the (alignment) training data’s diversity and augmentation, with results summarized in Table VIIIb. When training exclusively on respiratory sounds, performance on respiratory tasks sees a negligible change (0.786 vs. 0.788 AUROC), but performance on out-of-domain cardiac tasks drops significantly (0.661 vs. 0.601 AUROC). This demonstrates that training on

TABLE VIII: Summary of ablation studies. Each table reports the average performance over the three task categories. Respiratory and cardiac tasks use AUROC  $\uparrow$  (higher = better); lung-function tasks use MAE  $\downarrow$  (lower = better).

(a) Adaptation Data			(b) Data Augmentation			(c) Alignment		
Task Category	Resp. only	All	Task Category	With	Without	Task Category	Last-L	Multi-B
Resp. health $\uparrow$	0.788	0.786	Resp. health $\uparrow$	0.786	0.761	Resp. health $\uparrow$	0.786	0.784
Lung-function $\downarrow$	0.820	0.821	Lung-function $\downarrow$	0.821	0.973	Lung-function $\downarrow$	0.821	0.802
Cardiac condition $\uparrow$	0.601	0.661	Cardiac condition $\uparrow$	0.661	0.646	Cardiac condition $\uparrow$	0.661	0.659

TABLE IX: Ablation on masked-reconstruction loss (**Mask-Rec**) and alignment loss (**Align**) with a *pre-trained* model. The fourth row swaps our alignment loss (i.e., CKA-based) for an  $\ell^2$  (MSE) loss (marked  $\dagger$ ). The first row (no check-mark in “Pre-trained”) represents randomly initialized audio encoder but applies both losses.

Mask-Rec	Align	Pre-trained	Respiratory health $\uparrow$	Lung function $\downarrow$	Cardiac condition $\uparrow$
$\checkmark$	$\checkmark$		0.641	1.021	0.532
$\checkmark$		$\checkmark$	0.715	0.904	0.591
	$\checkmark$	$\checkmark$	0.768	0.865	0.645
$\checkmark$	$\checkmark^\dagger$	$\checkmark$	0.769	0.836	0.652
$\checkmark$	$\checkmark$	$\checkmark$	0.786	0.821	0.661

a large and diverse acoustic corpus is crucial for building a robust, generalizable model, even when the target application is domain-specific. Removing data augmentation reveals its critical role, especially for regression. While classification performance sees a modest decline, the MAE for lung function estimation increases dramatically from 0.821 to 0.973. This suggests that augmentation forces the model to learn features that are invariant to superficial recording variations (like volume), which is essential for predicting precise continuous values. A full per-task comparison is provided in Appendix G.

**Alignment Strategy.** We compare two alignment strategies: aligning only the final transformer layer (Last-L) versus multiple intermediate layers (Multi-B). As shown in Table VIIIc, the simpler single-layer approach is generally superior or comparable. The multi-layer approach offers no consistent benefit, indicating that the final layer of the LLMs already contains a sufficiently rich and compressed representation for semantic alignment. A task-wise breakdown is given in Appendix H.

**Loss Component Analysis.** We ablate the contributions of our dual-objective function components. As shown in Table IX, both the masked reconstruction loss (Mask-Rec) and alignment loss (Align) contribute to final performance, with the alignment loss proving more critical.

Removing masked reconstruction while keeping alignment results in modest degradation: respiratory condition inference drops from 0.786 to 0.768 AUROC, lung function estimation worsens from 0.821 to 0.865 MAE, and cardiac inference decreases from 0.661 to 0.645 AUROC. In contrast, removing alignment loss while keeping masked reconstruction causes larger performance drops across all categories: respiratory (0.786 to 0.715), lung function (0.821 to 0.904 MAE), and cardiac (0.661 to 0.591).

Furthermore, we examine alternative alignment objectives. Using  $\ell^2$  (MSE) loss instead of CKA for alignment (marked  $\dagger$ ) results in slightly worse performance across all metrics, validating our choice of CKA. Finally, training from random

weights instead of a pre-trained model catastrophically degrades performance (last row).

These results demonstrate that the CKA-based alignment loss is the primary driver for instilling semantic understanding, while masked reconstruction acts as a valuable regularizer that prevents the audio encoder from forgetting its acoustic modeling capabilities during alignment.

## VI. CONCLUSION

In this work, we demonstrate that pre-trained large language models can serve as effective “semantic teachers” to instill deep clinical understanding into specialized audio encoders. We introduced AcuLa, a general, lightweight alignment framework that successfully grounds high-level medical concepts from text into the fine-grained, temporal patterns of cardio-respiratory sounds. Our comprehensive experiments show that this fusion of semantic knowledge and acoustic modeling creates representations that are not only superior across a diverse range of 18 classification and regression tasks but are also more robust and clinically relevant. Our work establishes a novel direction for cross-modal learning, inverting the traditional knowledge flow to enhance perceptual models with abstract semantics. While our data generation strategy offers a scalable solution to leverage metadata for clinical text scarcity problem, the true promise lies in deploying this paradigm in data-rich clinical environments. Future work could extend this teacher-student paradigm to other physiological time-series like EEG and ECG, or develop self-correction cycles where model-disagreements flag cases for human-in-the-loop review, moving towards AI systems that truly reason about clinical data.

## ACKNOWLEDGMENTS

This work was supported by the NWO AiNed Fellowship Grant of A.S. We also acknowledge the use of the Dutch National Supercomputer Snellius for essential computational tasks.



## REFERENCES

- [1] A. Radford, J. W. Kim, C. Hallacy, A. Ramesh, G. Goh, S. Agarwal, G. Sastry, A. Askell, P. Mishkin, J. Clark *et al.*, “Learning transferable visual models from natural language supervision,” in *International conference on machine learning*. PMLR, 2021, pp. 8748–8763.
- [2] V. W. Liang, Y. Zhang, Y. Kwon, S. Yeung, and J. Y. Zou, “Mind the gap: Understanding the modality gap in multi-modal contrastive representation learning,” *Advances in Neural Information Processing Systems*, vol. 35, pp. 17 612–17 625, 2022.
- [3] A. Ray, F. Radenovic, A. Dubey, B. Plummer, R. Krishna, and K. Saenko, “Cola: A benchmark for compositional text-to-image retrieval,” *Advances in Neural Information Processing Systems*, vol. 36, pp. 46 433–46 445, 2023.
- [4] Y. Chen, J. Yuan, Y. Tian, S. Geng, X. Li, D. Zhou, D. N. Metaxas, and H. Yang, “Revisiting multimodal representation in contrastive learning: from patch and token embeddings to finite discrete tokens,” in *Proceedings of the IEEE/CVF Conference on Computer Vision and Pattern Recognition*, 2023, pp. 15 095–15 104.
- [5] J. Lee, J. Kim, H. Shon, B. Kim, S. H. Kim, H. Lee, and J. Kim, “Uni-clip: Unified framework for contrastive language-image pre-training,” *Advances in Neural Information Processing Systems*, vol. 35, pp. 1008–1019, 2022.
- [6] S. Yamaguchi, D. Feng, S. Kanai, K. Adachi, and D. Chijiwa, “Post-pre-training for modality alignment in vision-language foundation models,” in *Proceedings of the Computer Vision and Pattern Recognition Conference*, 2025, pp. 4256–4266.
- [7] Y. Gan, K. I. Zhao, and P. Isola, “Cross-modal alignment regularization: Enhancing language models with vision model representations,” in *Second Workshop on Representational Alignment at ICLR 2025*.
- [8] Y. Zhang, T. Xia, J. Han, Y. Wu, G. Rizos, Y. Liu, M. Mosuily, J. Ch, and C. Mascolo, “Towards open respiratory acoustic foundation models: Pretraining and benchmarking,” *Advances in Neural Information Processing Systems*, vol. 37, pp. 27 024–27 055, 2024.
- [9] Y. Zhang, T. Xia, A. Saeed, and C. Mascolo, “Respllm: Unifying audio and text with multimodal llms for generalized respiratory health prediction,” *arXiv preprint arXiv:2410.05361*, 2024.
- [10] B. Elizalde, S. Deshmukh, M. Al Ismail, and H. Wang, “Clap learning audio concepts from natural language supervision,” in *ICASSP 2023-2023 IEEE International Conference on Acoustics, Speech and Signal Processing (ICASSP)*. IEEE, 2023, pp. 1–5.
- [11] A. Guzhov, F. Raue, J. Hees, and A. Dengel, “Audioclip: Extending clip to image, text and audio,” in *ICASSP 2022-2022 IEEE International Conference on Acoustics, Speech and Signal Processing (ICASSP)*. IEEE, 2022, pp. 976–980.
- [12] Z. Borsos, R. Marinier, D. Vincent, E. Kharitonov, O. Pietquin, M. Sharifi, D. Roblek, O. Teboul, D. Grangier, M. Tagliasacchi *et al.*, “Audiolm: a language modeling approach to audio generation,” *IEEE/ACM transactions on audio, speech, and language processing*, vol. 31, pp. 2523–2533, 2023.
- [13] F. Kreuk, G. Synnaeve, A. Polyak, U. Singer, A. Défossez, J. Copet, D. Parikh, Y. Taigman, and Y. Adi, “Audiogen: Textually guided audio generation,” *arXiv preprint arXiv:2209.15352*, 2022.
- [14] G. Hinton, O. Vinyals, and J. Dean, “Distilling the knowledge in a neural network,” *arXiv preprint arXiv:1503.02531*, 2015.
- [15] W. Tan, H. Inaguma, N. Dong, P. D. Tomasello, and X. Ma, “SSR: Alignment-aware modality connector for speech language models,” in *Proceedings of the 22nd International Conference on Spoken Language Translation (IWSLT 2025)*, E. Salesky, M. Federico, and A. Anastasopoulos, Eds. Vienna, Austria (in-person and online): Association for Computational Linguistics, Jul. 2025, pp. 56–75. [Online]. Available: <https://aclanthology.org/2025.iwslt-1.5/>
- [16] T. Yu, H. Gao, T.-E. Lin, M. Yang, Y. Wu, W. Ma, C. Wang, F. Huang, and Y. Li, “Speech-text pre-training for spoken dialog understanding with explicit cross-modal alignment,” in *Proceedings of the 61st Annual Meeting of the Association for Computational Linguistics (Volume 1: Long Papers)*, A. Rogers, J. Boyd-Graber, and N. Okazaki, Eds. Toronto, Canada: Association for Computational Linguistics, Jul. 2023, pp. 7900–7913. [Online]. Available: <https://aclanthology.org/2023.acl-long.438/>
- [17] R. Girdhar, A. El-Nouby, Z. Liu, M. Singh, K. V. Alwala, A. Joulin, and I. Misra, “Imagebind: One embedding space to bind them all,” in *Proceedings of the IEEE/CVF conference on computer vision and pattern recognition*, 2023, pp. 15 180–15 190.
- [18] S. Kornblith, M. Norouzi, H. Lee, and G. Hinton, “Similarity of neural network representations revisited,” in *International conference on machine learning*. PMIR, 2019, pp. 3519–3529.
- [19] L. Jing, P. Vincent, Y. LeCun, and Y. Tian, “Understanding dimensional collapse in contrastive self-supervised learning,” *arXiv preprint arXiv:2110.09348*, 2021.
- [20] P.-Y. Huang, H. Xu, J. Li, A. Baevski, M. Auli, W. Galuba, F. Metze, and C. Feichtenhofer, “Masked autoencoders that listen,” *Advances in Neural Information Processing Systems*, vol. 35, pp. 28 708–28 720, 2022.
- [21] A. Saeed, D. Grangier, and N. Zeghidour, “Contrastive learning of general-purpose audio representations,” in *ICASSP 2021-2021 IEEE International Conference on Acoustics, Speech and Signal Processing (ICASSP)*. IEEE, 2021, pp. 3875–3879.
- [22] OpenAI, “Gpt-4 technical report,” 2024.
- [23] Z. Sun, “ICBHI 2017 challenge,” 2023.
- [24] J. Oliveira, F. Renna, P. D. Costa, M. Nogueira, C. Oliveira, C. Ferreira, A. Jorge, S. Mattos, T. Hatem, T. Tavares *et al.*, “The circo digiscope dataset: from murmur detection to murmur classification,” *IEEE journal of biomedical and health informatics*, vol. 26, no. 6, pp. 2524–2535, 2021.
- [25] F. Eyben, M. Wöllmer, and B. Schuller, “Opensmile: the munich versatile and fast open-source audio feature extractor,” in *Proceedings of the 18th ACM international conference on Multimedia*, 2010, pp. 1459–1462.
- [26] Google. (2025) MedGEMMA release. [Online]. Available: <https://huggingface.co/collections/google/medgemma-release-680aade845f90bec6a3f60c4>
- [27] Z. Papakipos and J. Bitton, “Augly: Data augmentations for robustness,” *arXiv preprint arXiv:2201.06494*, 2022.
- [28] M. Douze, A. Guzhva, C. Deng, J. Johnson, G. Szilvasy, P.-E. Mazaré, M. Lomeli, L. Hosseini, and H. Jégou, “The faiss library,” *arXiv preprint arXiv:2401.08281*, 2024.
- [29] M. Günther, S. Sturua, M. K. Akram, I. Mohr, A. Ungureanu, S. Eslami, S. Martens, B. Wang, N. Wang, and H. Xiao, “jina-embeddings-v4: Universal embeddings for multimodal multilingual retrieval,” 2025. [Online]. Available: <https://arxiv.org/abs/2506.18902>
- [30] H. Touvron, T. Lavril, G. Izacard, X. Martinet, M.-A. Lachaux, T. Lacroix, B. Rozière, N. Goyal, E. Hambro, F. Azhar *et al.*, “Llama: Open and efficient foundation language models,” *arXiv preprint arXiv:2302.13971*, 2023.
- [31] D. Guo, D. Yang, H. Zhang, J. Song, R. Zhang, R. Xu, Q. Zhu, S. Ma, P. Wang, X. Bi *et al.*, “Deepseek-r1: Incentivizing reasoning capability in llms via reinforcement learning,” *arXiv preprint arXiv:2501.12948*, 2025.
- [32] Kyutai. (2025) Helium 1: a modular and multilingual llm. [Online]. Available: <https://huggingface.co/collections/kyutai/helium-1-681237bbba8c1cf18a02e4bd>
- [33] L. B. Allal, A. Lozhkov, E. Bakouch, G. M. Blázquez, L. Tunstall, A. Piqueres, A. Marafioti, C. Zakka, L. von Werra, and T. Wolf, “Smolm2 - with great data, comes great performance,” 2024.
- [34] J. B. *et al.*, “Qwen technical report,” *arXiv preprint arXiv:2309.16609*, 2023.

## APPENDIX A

### PROMPT EXAMPLE FOR SYNTHETIC DATA GENERATION

Generating synthetic clinical reports is essential to the dataset construction process, as it enables the creation of diverse training data while maintaining clinical validity. The prompt presented here instructs the language model to adopt the role of a specialist physician interpreting auscultation findings. By restricting the output to factual descriptions of the given conditions and explicitly prohibiting recommendations for further evaluation, the prompt ensures that generated reports remain focused on objective clinical observations, mirroring real-world diagnostic documentation practices.

#### Off-the-shelf LLM Prompt for Data Generation

You are a <Pulmonologist/Cardiologist> tasked with interpreting <respiratory/cardiac> auscultation findings. Based on the given conditions, write 2–3 lines report covering all clinically relevant information. Only use the information given to write about conditions. Please do NOT mention anything about further evaluation or characterization.

Your output should be JSON of the following format: {'report': ...}

## APPENDIX B

### EXAMPLES OF METADATA–REPORT PAIRS

To illustrate the supervision signal used during alignment, Table X provides representative examples of paired metadata and generated reports across all datasets. Each report is produced under strict schema constraints and is limited to restating clinician-verified fields without adding diagnostic speculation. These examples demonstrate how the LLM transforms structured metadata into concise, clinically grounded descriptions suitable for semantic alignment.

Dataset	Metadata (clinician-verified)	LLM-generated clinical report
ICBHI	Chest_Location: Trachea; Crackles: No; Wheezes: Yes; Age: 66.0; Sex: M; Diagnosis: Pneumonia.	<i>Auscultation over the trachea reveals wheezes without crackles in this 66-year-old male diagnosed with pneumonia. The presence of wheezing over the tracheal area is consistent with airway involvement in the documented pneumonia.</i>
HFLung	Sound_type: Normal; Sound: Normal; Device: Littmann 3200.	<i>Normal vesicular breath sounds are heard bilaterally using the Littmann 3200 device, with no adventitious sounds detected. These findings are consistent with normal respiratory function.</i>
UK Covid-19	Age: 18–44; Gender: Female; Covid_Test_Result: Positive; Symptom_Sore_throat: Yes; Symptom_Shortness_of_breath: No; Symptom_Runny_or_blocked_nose: Yes; Symptom_New_continuous_cough: Yes; Symptom_Fatigue: Yes; Symptom_Headache: Yes; Symptom_Loss_of_Taste: No; Smoker_status: Never smoked.	<i>Respiratory auscultation in this COVID-19 positive young adult female reflects a symptom profile including sore throat, runny or blocked nose, continuous cough, fatigue, and headache, with no reported shortness of breath or loss of taste. These observations align with the provided metadata and indicate symptomatic COVID-19 without additional reported complications.</i>
CoughVID	Age: 15.0; Gender: Male; Respiratory_Condition: False; Fever/Muscle_Pain: False; Status: Healthy.	<i>Clear breath sounds are heard bilaterally without wheezes, crackles, or rhonchi in this healthy 15-year-old male. The respiratory examination is unremarkable and consistent with normal pulmonary findings.</i>
Circor	Murmur: Present; Murmur_locations: AV+MV+PV+TV; Most audible location: MV; Timing: Holosystolic; Shape: Plateau; Grading: II/VI; Pitch: Medium; Quality: Harsh; Outcome: Abnormal.	<i>A holosystolic, medium-pitched murmur with a harsh quality and plateau shape is heard most clearly at the mitral valve area and is also audible at the aortic, pulmonic, and tricuspid positions. The murmur is graded II/VI, indicating an abnormal cardiac finding.</i>
SPRSound	Record_Annotation: Continuous & Discontinuous Adventitious Sounds; Event_Type: Wheeze; Disease: Pneumonia (severe)	<i>The auscultation reveals the presence of both continuous and discontinuous adventitious sounds indicative of severe pneumonia. Wheezing is noted, which may suggest obstructive airway pathology or reactive airway process in the context of this illness.</i>
ZCHSound	Diagnosis: Normal; Data_Type: Clean.	<i>Cardiac auscultation reveals normal heart sounds with a regular rhythm and no audible murmurs, rubs, or gallops, consistent with a normal cardiac examination.</i>

TABLE X: Examples of clinician-verified metadata and the corresponding LLM-generated clinical reports across all datasets. Each generated report is a schema-constrained restatement of the metadata fields, ensuring factual fidelity and preventing the introduction of new diagnoses or speculative clinical reasoning.

## APPENDIX C

### OPENSIMILE BASELINE RESULTS

We compare our method with OpenSmile, a handcrafted-feature baseline. Our approach consistently outperforms it across all tasks, with especially strong gains on complex diagnostic settings.

TABLE XI: Comparison of OpenSmile baseline with our approach. AUROC is reported for classification tasks (T1-T9, higher is better) and MAE for regression tasks (T10-T16, lower is better). We report mean and standard deviation from five independent runs for classification tasks and across subjects for regression tasks.

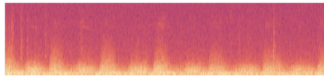
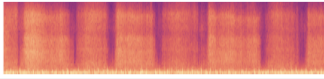
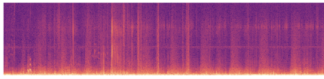
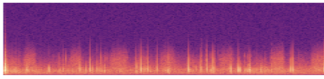
ID	Task	OpenSmile	AcuLa (Ours)
<b>Classification Tasks (AUROC)</b>			
T1	Covid (Exhale)	0.550 $\pm$ 0.015	0.698
T2	Covid (Cough)	0.649 $\pm$ 0.006	0.730
T3	Covid (Cough)	0.537 $\pm$ 0.011	0.887
T4	Gender (Cough)	0.677 $\pm$ 0.005	0.796
T5	COPD (Lung)	0.579 $\pm$ 0.043	0.826
T6	Smoker (Cough)	0.534 $\pm$ 0.060	0.830
T7	Gender (Cough)	0.753 $\pm$ 0.008	0.845
T8	Obstructive (Lung)	0.636 $\pm$ 0.082	0.752
T9	COPD severity (Lung)	0.494 $\pm$ 0.054	0.710
<b>Regression Tasks (MAE)</b>			
T10	FVC (Breath)	0.985 $\pm$ 0.743	0.865
T11	FEV1 (Breath)	0.756 $\pm$ 0.721	0.742
T12	FEV1/FVC (Breath)	0.141 $\pm$ 0.185	0.127
T13	FVC (Vowel)	0.850 $\pm$ 0.592	0.779
T14	FEV1 (Vowel)	0.730 $\pm$ 0.497	0.725
T15	FEV1/FVC (Vowel)	0.138 $\pm$ 0.166	0.123
T16	Breathing Rate	2.714 $\pm$ 0.902	2.388

## APPENDIX D

### QUALITATIVE RETRIEVAL EXAMPLES

This section provides representative query cases (Figure 4). Each row shows the query spectrogram and report with the top three FAISS-retrieved reports. The retrieved texts capture the key findings, demonstrating that the shared embedding space preserves fine-grained diagnostic cues.

Fig. 4: Top-3 clinical reports retrieved for auscultation clips. Left: query spectrogram+reference report. Right: three closest matches returned by our audio-text model.

Original Report	Closest Reports
<p>Respiratory auscultation reveals normal vesicular breath sounds without evidence of added sounds such as crackles, wheezes, or rhonchi. There are no signs of respiratory distress or abnormal auscultatory findings.</p> 	<ol style="list-style-type: none"> <li>1. Normal vesicular breath sounds are heard bilaterally with no added sounds such as crackles, wheezes, or rhonchi. No signs of respiratory distress or abnormal auscultatory findings.</li> <li>2. Normal vesicular breath sounds are heard bilaterally with no adventitious sounds such as wheezes, crackles, or rhonchi. There are no areas of decreased breath sounds or abnormal bronchial breathing.</li> <li>3. Auscultation reveals clear breath sounds bilaterally with normal vesicular pattern and no adventitious sounds. No wheezes, crackles, or abnormal findings detected.</li> </ol>
<p>The presence of continuous adventitious sounds, specifically rhonchi, suggests airway obstruction potentially due to mucus or airway constriction commonly associated with conditions such as bronchitis or chronic obstructive pulmonary disease (COPD).</p> 	<ol style="list-style-type: none"> <li>1. The presence of continuous adventitious sounds, diagnosed as wheezes, suggests airflow obstruction which may be associated with conditions such as asthma, chronic obstructive pulmonary disease (COPD), or bronchitis.</li> <li>2. The respiratory examination reveals continuous adventitious sounds, characterized by rhonchi and wheeze, which may indicate bronchial obstruction or airway narrowing, commonly associated with conditions such as COPD or asthma.</li> <li>3. The presence of continuous adventitious sounds identified as rhonchi suggests airway obstruction or secretions in larger airways, typically associated with conditions like chronic bronchitis or pneumonia.</li> </ol>
<p>On auscultation, there are focal inspiratory crackles in the lower left lung field without evidence of wheezing or rhonchi. Findings are consistent with a localized consolidation pattern.</p> 	<ol style="list-style-type: none"> <li>1. On auscultation, there are focal inspiratory crackles localized over the right lower lung field, with bronchial breath sounds present in the same area. No wheezes or pleural rubs detected. These findings are consistent with a localized pulmonary process such as consolidation.</li> <li>2. On auscultation, breath sounds reveal inspiratory crackles localized to the lower lung fields, with reduced air entry. No evidence of wheezing or rhonchi is present.</li> <li>3. Breath sounds may be normal or show mild bilateral crackles at lung bases, with no evidence of wheezing or rhonchi. There are no pleural rubs or focal consolidations detected.</li> </ol>
<p>Expiratory wheezes are detected in the anterior right upper lung field of a 46-year-old male with asthma, indicating airway narrowing or obstruction typically associated with this condition.</p> 	<ol style="list-style-type: none"> <li>1. The respiratory auscultation reveals expiratory wheezes in the posterior right middle lung field, consistent with obstructive airways typically observed in asthma. This finding in a 43-year-old female is indicative of airway narrowing or bronchospasm.</li> <li>2. The presence of expiratory wheezes over the posterior right lower lung region in this 58-year-old female with COPD may indicate airway obstruction or inflammation, commonly associated with this condition.</li> <li>3. Expiratory wheezes are noted in the anterior right upper lung field, consistent with asthma in this 46-year-old male.</li> </ol>

## APPENDIX E

### COMPARISON OF DIFFERENT LLMs

We compare our approach against OpenSmile, a standard baseline that relies on handcrafted acoustic features. The results demonstrate consistent performance improvements across all tasks and reveal the advantages of learned representations over traditional feature engineering for medical audio analysis. Our method achieves particularly strong gains on complex diagnostic tasks, where capturing subtle acoustic patterns is essential for accurate classification.

TABLE XII: Comparison of different LLMs across respiratory and cardiac audio tasks. T1-T9: respiratory classification (AUROC), T10-T16: lung function estimation (MAE), T17-T18: cardiac classification (AUROC).

ID	Task	MedGemma-4B	Llama-3.2-3B	DS-R1-DQ-1.5B	Helium 2B	SmolLM2
T1	Covid / Non-covid (Exhalation)	0.698	0.671	0.633	0.645	0.588
T2	Covid / Non-covid (Cough)	0.730	0.685	0.646	0.650	0.611
T3	Covid / Non-covid (Cough)	0.887	0.789	0.753	0.726	0.708
T4	Female / Male (Cough)	0.796	0.804	0.733	0.701	0.692
T5	COPD / Healthy (Lung sounds)	0.826	0.773	0.758	0.765	0.736
T6	Smoker / Non-smoker (Cough)	0.830	0.750	0.693	0.718	0.708
T7	Female / Male (Cough)	0.845	0.824	0.836	0.787	0.769
T8	Obstructive / Healthy (Lung sounds)	0.752	0.649	0.643	0.625	0.609
T9	COPD severity (Lung sounds)	0.710	0.632	0.627	0.610	0.594
T10	FVC (Breath)	0.865	0.895	0.976	0.910	0.917
T11	FEV1 (Breath)	0.742	0.786	0.825	0.857	0.889
T12	FEV1/FVC (Breath)	0.127	0.131	0.136	0.145	0.142
T13	FVC (Vowel)	0.779	0.830	0.885	0.901	0.915
T14	FEV1 (Vowel)	0.725	0.750	0.804	0.837	0.855
T15	FEV1/FVC (Vowel)	0.123	0.133	0.139	0.135	0.139
T16	Breathing Rate	2.388	2.445	2.507	2.565	2.641
T17	Murmur / Healthy	0.675	0.626	0.670	0.590	0.641
T18	Symptomatic / Healthy	0.647	0.652	0.645	0.618	0.630

## APPENDIX F

### PERFORMANCE OF A RESPIRATORY-ONLY MODEL ON RESPIRATORY AND CARDIAC AUDIO TASKS

We evaluate the performance of a model trained exclusively on respiratory audio data across both respiratory and cardiac tasks. The model maintains strong performance on respiratory-specific tasks (T1-T16), achieving comparable results to our multi-organ trained model. However, performance degrades on cardiac classification tasks (T17-T18), with AUROC scores dropping to approximately 0.6.

TABLE XIII: Performance on respiratory and cardiac audio tasks using model trained exclusively on respiratory sounds data. T1-T9: respiratory classification (AUROC), T10-T16: lung function estimation (MAE), T17-T18: cardiac classification (AUROC).

ID	Task	MedGemma-4B
T1	Covid / Non-covid (Exhalation)	0.695
T2	Covid / Non-covid (Cough)	0.748
T3	Covid / Non-covid (Cough)	0.885
T4	Female / Male (Cough)	0.793
T5	COPD / Healthy (Lung sounds)	0.823
T6	Smoker / Non-smoker (Cough)	0.838
T7	Female / Male (Cough)	0.850
T8	Obstructive / Healthy (Lung sounds)	0.745
T9	COPD severity (Lung sounds)	0.718
T10	FVC (Breath)	0.863
T11	FEV1 (Breath)	0.744
T12	FEV1/FVC (Breath)	0.118
T13	FVC (Vowel)	0.783
T14	FEV1 (Vowel)	0.717
T15	FEV1/FVC (Vowel)	0.124
T16	Breathing Rate	2.391
T17	Murmur / Healthy	0.605
T18	Symptomatic / Healthy	0.597

## APPENDIX G

### RESPIRATORY AND CARDIAC AUDIO PERFORMANCE WITHOUT AUGMENTATION

We investigate the impact of data augmentation during the alignment phase by evaluating model performance without any augmentation. The results show consistent performance degradation across most tasks compared to our augmented approach. Classification tasks experience AUROC reductions of 0.02-0.05, while regression tasks show increased MAE values, particularly for FEV1/FVC estimation.

TABLE XIV: Performance on respiratory and cardiac audio tasks without data augmentation during alignment. T1-T9: respiratory classification (AUROC), T10-T16: lung function estimation (MAE), T17-T18: cardiac classification (AUROC).

ID	Task	MedGemma-4B
T1	Covid / Non-covid (Exhalation)	0.652
T2	Covid / Non-covid (Cough)	0.691
T3	Covid / Non-covid (Cough)	0.864
T4	Female / Male (Cough)	0.782
T5	COPD / Healthy (Lung sounds)	0.798
T6	Smoker / Non-smoker (Cough)	0.825
T7	Female / Male (Cough)	0.833
T8	Obstructive / Healthy (Lung sounds)	0.728
T9	COPD severity (Lung sounds)	0.673
T10	FVC (Breath)	0.908
T11	FEV1 (Breath)	0.779
T12	FEV1/FVC (Breath)	0.135
T13	FVC (Vowel)	0.807
T14	FEV1 (Vowel)	0.745
T15	FEV1/FVC (Vowel)	1.122
T16	Breathing Rate	2.318
T17	Murmur / Healthy	0.665
T18	Symptomatic / Healthy	0.627

## APPENDIX H

### ALIGNMENT STRATEGY ANALYSIS

We compare two alignment strategies: aligning only the final transformer layer (Last-L) versus multiple intermediate layers (Multi-L at blocks 3, 6, 9, 12). Last-L generally outperforms Multi-L, especially in classification tasks. This suggests that aligning only the final layer better preserves hierarchical feature learning and allows more flexible, task-specific representations.

TABLE XV: Single-layer vs. multi-layer alignment on each downstream task. **Last-L** = alignment applied *only* to the final transformer block; **Multi-L** = alignment applied to blocks {3, 6, 9, last (12)}, with the four alignment losses averaged. T1-T9: respiratory classification (AUROC), T10-T16: lung function estimation (MAE), T17-T18: cardiac classification (AUROC).

ID	Task	Last-L	Multi-B
T1	Covid / Non-covid (Exhalation)	0.698	0.694
T2	Covid / Non-covid (Cough)	0.730	0.742
T3	Covid / Non-covid (Cough)	0.887	0.879
T4	Female / Male (Cough)	0.796	0.774
T5	COPD / Healthy (Lung sounds)	0.826	0.820
T6	Smoker / Non-smoker (Cough)	0.830	0.817
T7	Female / Male (Cough)	0.845	0.818
T8	Obstructive / Healthy (Lung sounds)	0.752	0.770
T9	COPD severity (Lung sounds) <sup>1</sup>	0.710	0.744
T10	FVC (Breath)	0.865	0.840
T11	FEV1 (Breath)	0.742	0.715
T12	FEV1/FVC (Breath)	0.127	0.118
T13	FVC (Vowel)	0.779	0.742
T14	FEV1 (Vowel)	0.725	0.692
T15	FEV1/FVC (Vowel)	0.123	0.125
T16	Breathing Rate	2.388	2.385
T17	Murmur / Healthy	0.675	0.660
T18	Symptomatic / Healthy	0.647	0.657